Journal of Alloys and Compounds 509 (2011) 1989–1993

Contents lists available at ScienceDirect

Journal of Alloys and Compounds

journal homepage: www.elsevier.com/locate/jallcom

Structure and mechanical properties of Ti–Al–N coatings deposited by combined cathodic arc middle frequency magnetron sputtering

C.W. Zou [a], J. Zhang [a], W. Xie [a], L.X. Shao [a,*], D.J. Fu [b]

[a] Department of Physics and Development Center for New Materials Engineering & Technology in Universities of Guangdong, Zhanjiang Normal University, Zhanjiang, 524048, China
[b] Accelerator Laboratory, Department of Physics, Wuhan University, Wuhan, 430072, China

ARTICLE INFO

Article history:
Received 5 October 2010
Accepted 25 October 2010
Available online 4 November 2010

Keywords:
Ti–Al–N coatings
Microstructure
Hardness
Magnetron sputtering

ABSTRACT

Ti–Al–N coatings were deposited on Si (1 1 1) and WC substrates by combined cathodic arc middle-frequency magnetron (MF) sputtering under a Ti arc power of 10 kW and with different Al MF targets currents. X-ray diffraction patterns (XRD) showed that the Ti–Al–N coatings were polycrystallize with a preferred (1 1 1) orientation at $2\theta = 43.7^\circ$. The (1 1 1) diffraction showed a decrease in peak intensity but a increase in FWHM values with the increasing of Al contents. Nano-meter sized TiN crystal grains distinguished by the lattice fringe contrast were verified by plan-view transmission electron (TEM) and selected area electron diffraction (SAED) images. With the increasing of MF sputter currents from 5 to 20 A, the Al contents in the Ti–Al–N coatings monotonically increased from 4.8 to 10.8 at.%, whereas the N and O contents were nearly constant. The hardness of the Ti–Al–N coatings was in the range of 23–32 GPa, and the Young modulus values were in the range of 420–540 GPa.

© 2010 Elsevier B.V. All rights reserved.

1. Introduction

Much attention has been paid to the transition-metal nitride and carbide coatings in recent years due to their huge application potential on cutting tools and machine parts. These coatings have excellent properties such as high hardness, good adhesion to substrates and good resistance against wear and corrosion. Following successful industrial application of thin protective coatings, a lot of work has been done on nitride ternary alloy coatings, especially Ti–Al–N, because it could be applied as anti-oxidation on molding dies and as thick anti-wear coatings on automobile piston rings [1,2].

Ti–Al–N coatings are usually grown by cathode arc discharge, chemical vapor deposition, and reactive magnetron sputtering [3–5]. The magnetron sputtering has been extensively used because of its low level of liquid–particle ejection and materials consumption. Sputter systems equipped with twin magnetron targets powered by middle frequency of 20–80 kHz power supplies, which may effectively reduced target poisoning as the pair targets becomes cathode and anode alternatively, have been developed and industrially applied in high-rate deposition of protective coatings.

Previously, we have prepared Ti-containing a-C nanocomposite coatings, AlN and Ti–Si–N films [6–8]. The deposition rates were as high as 4 μm/h. In this paper we use a home-made arc-assisted MF machine to prepare and study the influence of Al targets currents on the microstructure, bond states and hardness values of the resulting Ti–Al–N coatings.

2. Experimental details

The Ti–Al–N coatings were deposited on Si (1 1 1) and WC substrate in a gas mixture of Ar and N_2 in a dual cathode MF reactive magnetron sputtering chamber equipped with an arc source. A pair of rectangle Al targets with a purity of 99.999% and a metal Ti target with a purity of 99.99% were mounted on the side wall of the chamber. Fig. 1 shows the schematic cross-sectional view of the combined cathodic arc MF magnetron sputtering system. One Ti target is run in cathodic arc mode while the rest two Al targets in MF magnetron sputtering mode. Before deposition, the substrates were cleaned ultrasonically in acetone and methanol and rinsed de-ionized water at 80 °C. After pumping the chamber to a pressure below 8×10^{-4} Pa, the substrates were etched for 30 min in Ar plasma at 2.0 Pa. The substrates were placed vertically on a rotating sample carrier, the sample experiences three-dimensional rotations, i.e., the sample carrier rotates around the chamber center, the carrier spins, and the sample spins. This improves the uniformity of the resulting coatings. The Al targets are powered with a 20 kW MF power supply and the metal Ti targets are powered with a 10 kW cathodic arc power supply. The base pressure prior to coating deposition was 8×10^{-4} Pa. During deposition, the substrates rotated in the chamber and faced the Ti target and Al targets sequentially. The

* Corresponding author. Tel.: +86 759 3183260; fax: +86 759 3183260.
E-mail address: Changweizou@hotmail.com (L.X. Shao).

0925-8388/$ – see front matter © 2010 Elsevier B.V. All rights reserved.
doi:10.1016/j.jallcom.2010.10.110

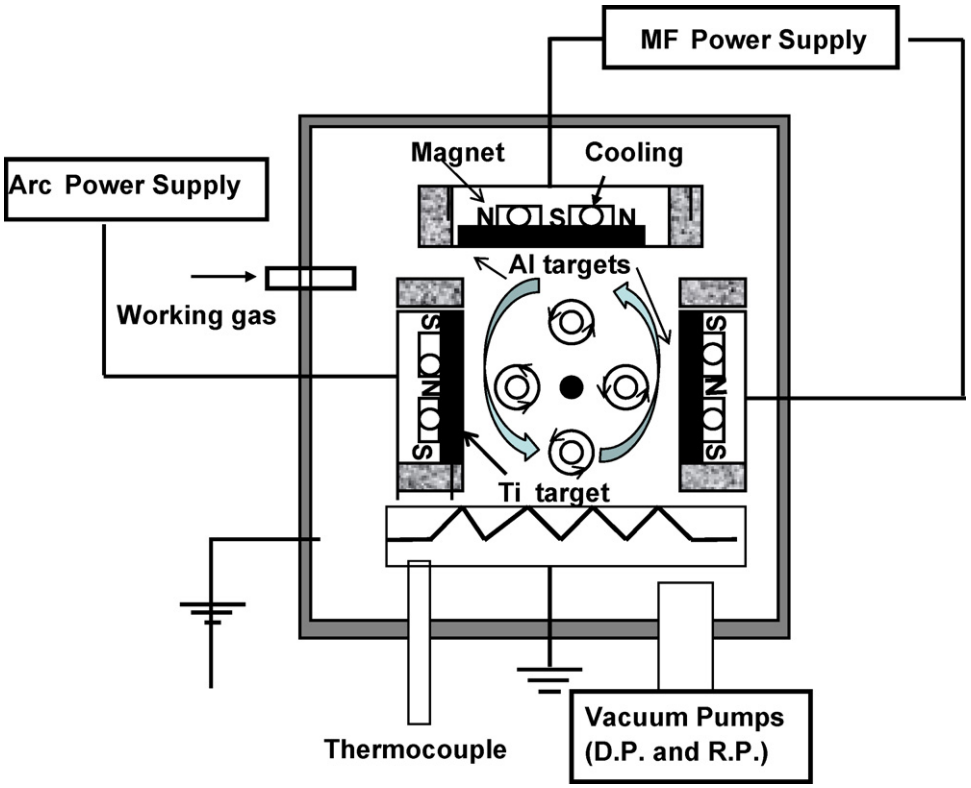

Fig. 1. Schematic diagram of the combined cathodic arc middle frequency magnetron sputtering system.

pulsed bias on the substrate is fixed at −150 V. The current passing the Al targets was varied between 5 and 20 A. The working pressure was kept at 0.4 Pa and the flow rate of N_2/Ar was fixed at 1:1. The substrate temperature was set at 400 °C and the duration of the coating process was 60 min.

The structure of the Ti–Al–N films was determined by X-ray diffraction (XRD, Bruker-axs D8 Advance) using Cu K_a radiation of a wavelength 0.154 nm. The root-mean-square (RMS) roughness was determined by atomic force microscopy (AFM, SPM-9500J3, Shimadzu) operated in taping mode with a measuring area of

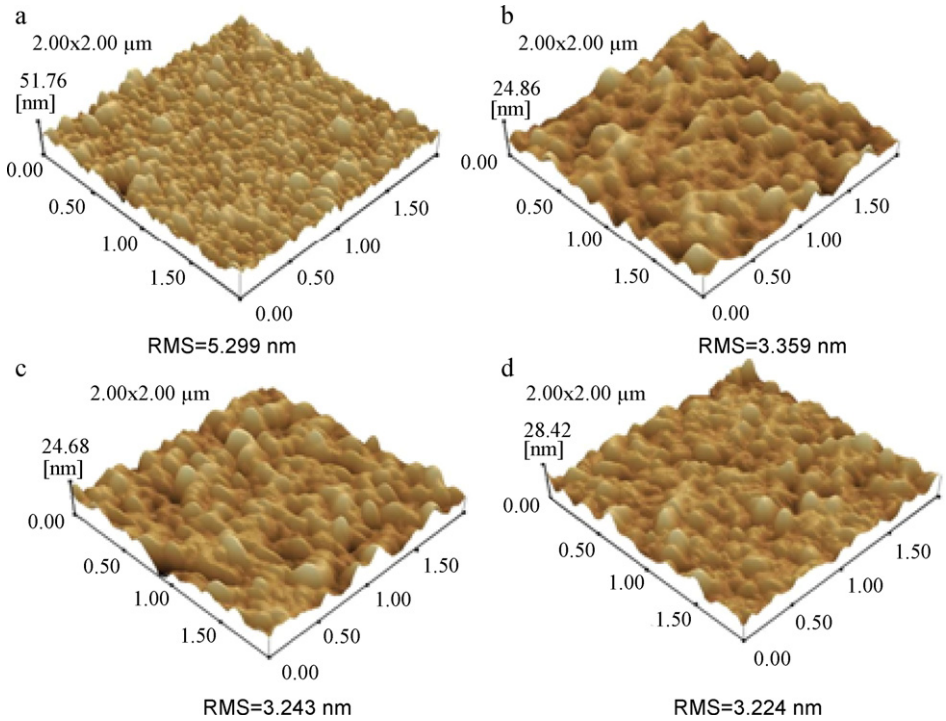

Fig. 2. AFM images of Ti–Al–N coatings deposited at Al target currents of 5 A (a), 10 A (b), 15 A (c) and 20 A (d), respectively.

2 μm × 2 μm. The surface morphology, cross-sectional structure and elemental composition were characterized by an FEI Sirion IMP SEM system equipped with an EDAX genesis 7000 energy dispersive spectrometer (EDS) operated at 12 kW. The thickness of the films was measured by a stylus profiler and confirmed by cross-sectional SEM. The hardness and Young's modulus were measured using a fully calibrated MTS Nano Indenter XP. In order to avoid surface and substrate effect, the depth of indentation was set at 100–200 nm which was lower than 10% of the film thickness. On each sample, ten separated measurements were taken to obtain a mean hardness.

3. Results and discussion

Fig. 2 shows the AFM images and RMS roughness values of Ti–Al–N coatings deposited at various Al targets currents. As can be seen from the figure, with the increasing of Al target currents from 5 to 20 A, a smoother surface was obtained. However, the RMS roughness was decreased to one-half in comparison with that achieved in the TiN films produced by the same method [9]. The average roughness values of the coatings deposited at Al targets currents of 5, 10, 15 and 20 A are 5.299, 3.359, 3.243, 3.224 nm, respectively. As the Al target currents increase, the grain and column boundaries become denser, and the smoother surface appears.

Fig. 3 shows the changes of Al contents in the Ti–Al–N coatings as a function of Al targets currents at a fixed Ti arc power supply of 10 kW. With the increasing of MF sputter currents from 5 to 20 A, the Al contents in the Ti–Al–N coatings monotonically increased from 4.8 to 10.8 at.%, whereas the N and O contents were nearly constant. Similar result has been achieved by Si in Ti–Si–C–N coatings by a hybrid deposition technique [10]. The EDS spectrum of Ti–Al–N

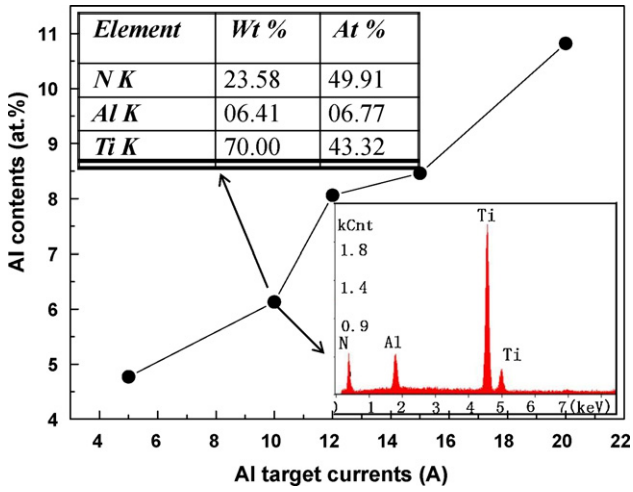

Fig. 3. Al contents in the Ti–Al–N coatings as a function of Al targets currents. Corresponding EDS images and elements ratio are shown in the inset.

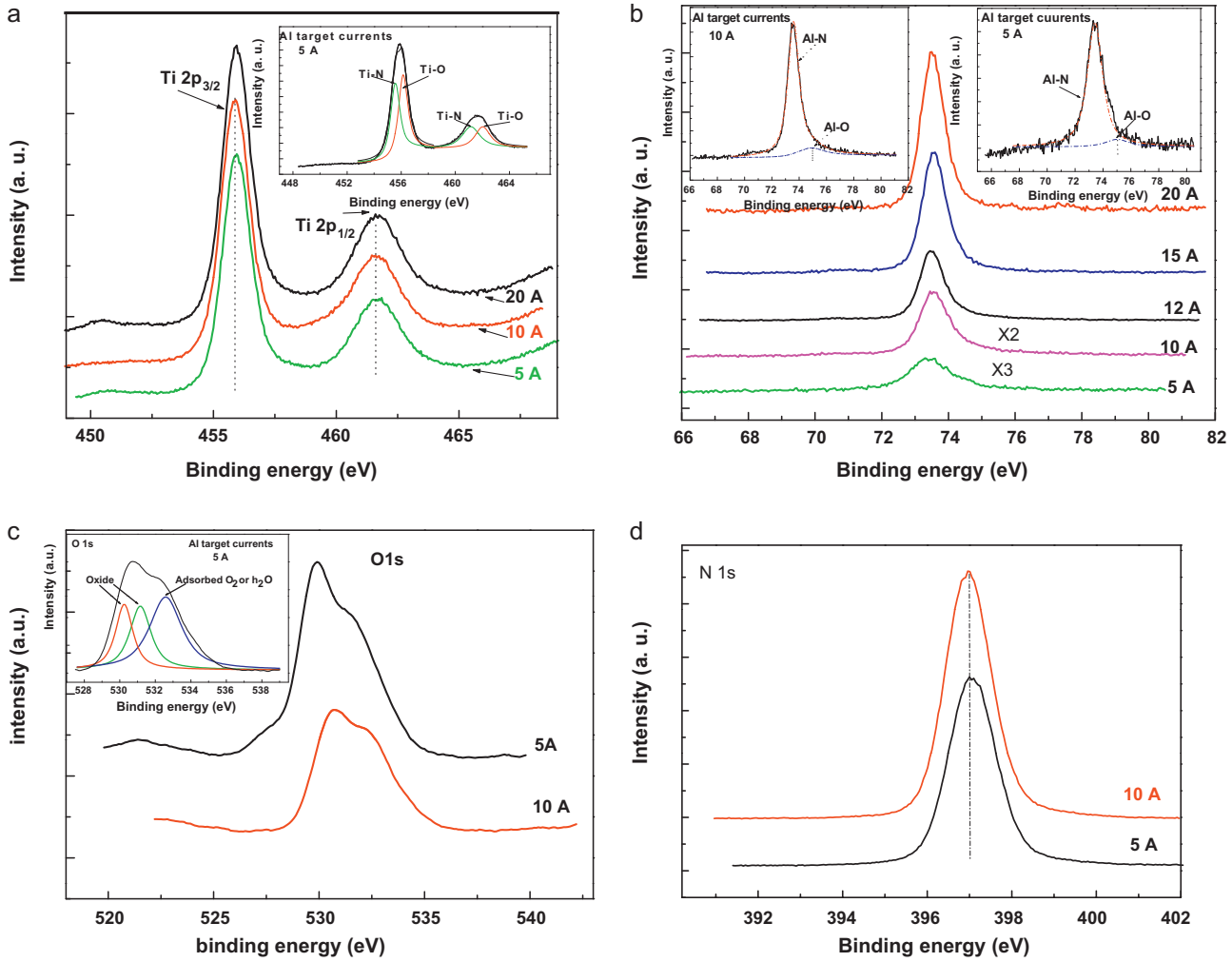

Fig. 4. XPS spectra of Ti–Al–N coatings deposited at various Al target currents: (a) Ti $2p_{3/2}$ and Ti $2p_{1/2}$, (b) Al 2p, (c) O 1s and (d) N 1s.

coatings produced at Al target currents of 10 A are shown in the inset and the corresponding N, Al and Ti contents are, respectively, 49.91, 6.77 and 43.32 at.%.

Fig. 4 gives the XPS analysis of the resulting Ti–Al–N coatings. The binding states of Ti 2p spectra shown in Fig. 4a are clearly resolved into two doublets peaks. The binding energy (BE) at low energy side ranging from 454 to 460 eV is corresponding to Ti $2p_{3/2}$ state. In this range, the low BE (~455.8 eV) is attributed to Ti–N (TiN) bonds and the high BE (~458.8 eV) as shown in inset of Fig. 4a can be assigned to Ti–O (TiO_2) bonds [11]. The corresponding Ti $2p_{1/2}$ states located at high energy side and doublets are shown in same color. Al 2p core level curves shown in Fig. 4b are fitted with two components, lower BE centered at 73.5 eV and higher BE located at about 75.6 eV. The lower BE of 73.5 eV is higher than metallic Al 2p 72.8 eV but lower than Al 2p 74.5 eV in AlN [12,13]. The shift of BE maybe attribute to the formed un-stoichiometric AlN compounds. Another higher BE located at about 75.6 eV can be attributed to Al–O bonds in α-Al_2O_3. Fig. 4c shows the O 1s core level spectrum. The O 1s spectrum can be fitted into three peaks located at 530, 532 and 533 eV, respectively. The BE of main two peaks (530 and 532 eV) can be assigned to oxides of Ti and Al, respectively. And the peak centered at 533 eV is related to the adsorbed oxygen or water molecules on the surface [14]. N 1s core level curves revealed in Fig. 4d are assigned to the nitrides of Ti and Al.

Fig. 5 shows the XRD patterns of Ti–Al–N coatings deposited at various Al target currents. The diffraction patterns exhibited a pattern of crystalline (Ti, Al)N with mixed orientation of (1 1 1), (2 0 0) and (2 2 0). With the increasing of Al targets currents, the preferred (1 1 1) orientation centered at $2\theta = 43.7^\circ$ showed a decrease in peak intensity but a increase FWHM (width at half maximum). Such a tendency of XRD peak broadening was reported to be due to grain

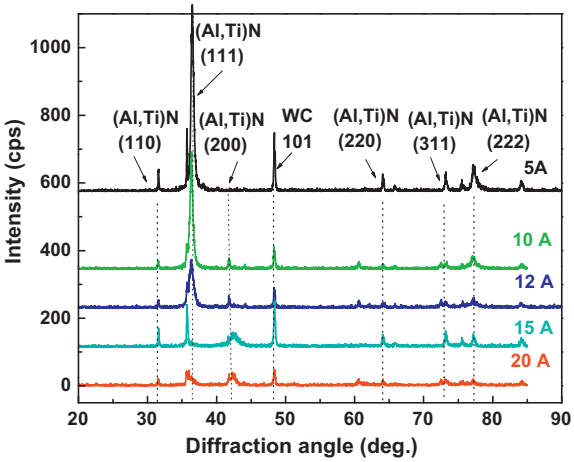

Fig. 5. XRD patterns of Ti–Al–N coatings deposited at various Al target currents.

size reduction [15]. And also, with the increasing of Al contents from 5 to 20 A, the peak position shifts to high 2θ values which indicated that the decrease in lattice parameter. This was due to the replacement of Ti atoms by the smaller Al atoms in the TiN lattice [16,17].

Plain view TEM images of Ti–Al–N coatings deposited at Al targets currents of 5 and 10 A were shown in Fig. 6a and b, respectively. Inset presented the typical selected area electron diffraction (SAED) pattern obtained from the corresponding samples. The Ti–Al–N films exhibit defined and continuous ring patterns which indicated nano-crystalline character of the films [17]. The nano-

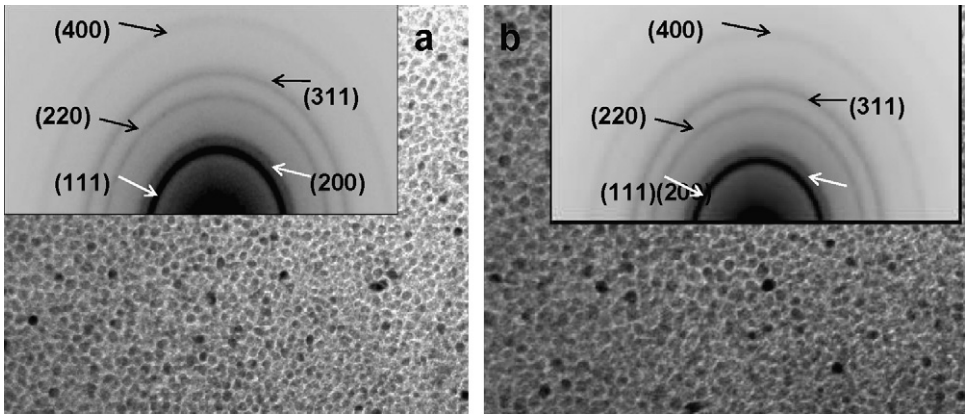

Fig. 6. TEM images of Ti–Al–N coatings deposited at Al targets currents of 5 A (a), and 10 A (b), respectively. The corresponding SAED patterns are shown in insets.

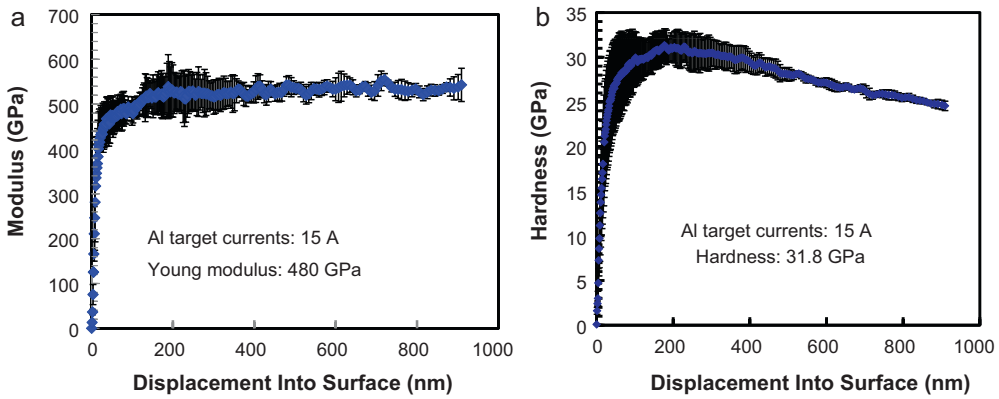

Fig. 7. Young modulus (a) and hardness (b) values as a function of displacement into surface for Ti–Al–N coatings deposited at Al target currents of 10 A.

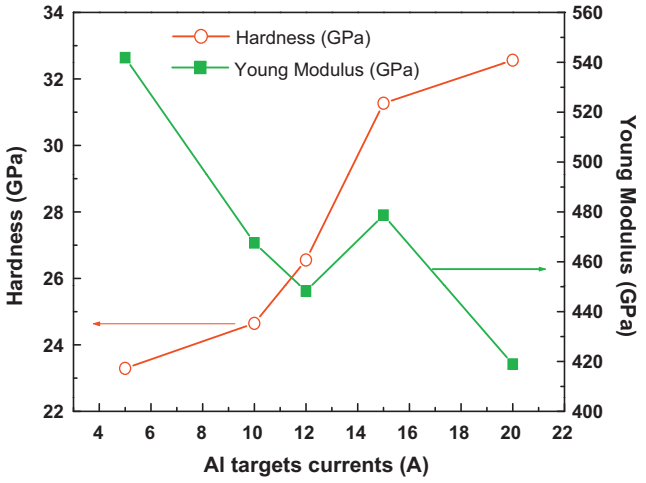

Fig. 8. Hardness and Young modulus of Ti–Al–N coatings as a function of Al target currents.

meter sized (2–3 nm) crystal grains, which are distinguished by the lattice fringe contrast, are clearly visible. SAED pattern of the coatings clearly shows the (1 1 1), (2 0 0), and (2 2 0) diffraction rings for the face-centered-cubic-like-B1-NaCl structure, which can be attributed to nano-crystalline Ti–Al–N solid solution. The solid solution of Ti–Al–N by adding Al into the growing TiN films has been confirmed by Shum et al. [18].

The hardness and Young modulus values as a function of displacement in coatings produced at Al targets currents of 15 A were shown in Fig. 7a and b. The hardness was measured by nano-indenter using a continuous stiffness methods applying continuous loading-unloading indentation which enable us to measure the continuous hardness of film initial indentation to final indentation depth [19]. The average values at the indentation depth of 75–100 nm were determined with the hardness (H) and elastic modulus (E) of each film, and these values are shown in Fig. 8. The hardness of the coatings gradually increased with the increasing of Al content and reached the maximum values of approximately 32.8 GPa at Al targets currents of 20 A. However, the elastic modulus of the Ti–Al–N coatings dropped rapidly with increase of Al content. This enhancement on the hardness properties could be attributed to the crystal size refinement. According to the Hall–Petch relationship [20], decreasing crystalline size of nano-crystalline materials increases the hardness of the materials [21].

4. Conclusion

We have studied the influence of Al targets currents on the structure and mechanical properties of Ti–Al–N coatings deposited on Si (1 1 1) and WC substrates by arc source assisted MF magnetron sputtering. Nano-meter sized TiN crystal grains distinguished by the lattice fringe contrast were verified by plan-view transmission electron (TEM) and selected area electron diffraction (SAED) images. The hardness of the coatings gradually increased with the increasing of Al contents and this enhancement on the hardness properties can be attributed to crystal size refinement.

Acknowledgement

This work was supported by the National Natural Science Foundation of China under contracts 10435060 and 10675095.

References

[1] F. Quesada, A. Marino, E. Restrepo, Surf. Coat. Technol. 201 (2006) 2925.
[2] S.Y. Yoon, J.K. Kim, K.H. Kim, Surf. Coat. Technol. 161 (2002) 237.
[3] T. Mashiki, H. Hikosaka, H. Tanoue, H. Takikawa, Y. Hasegawa, M. Taki, M. Kumagai, M. Kamiya, Thin Solid Films 516 (2008) 6650.
[4] S. Ikeda, S. Gilles, B. Chenevier, Thin Solid Films 315 (1998) 257.
[5] G.S. Kim, B.S. Kim, S.Y. Lee, J.H. Hahn, Thin Solid Films 1506 (2006) 128.
[6] B. Yang, Z.H. Huang, C.S. Liu, Z.Y. Zeng, X.J. Fan, D.J. Fu, Jpn. J. Appl. Phys. 44 (2005) 1022.
[7] C.W. Zou, M.L. Yin, M. Li, L.P. Guo, D.J. Fu, Appl. Surf. Sci. 253 (2007) 9077.
[8] M.L. Yin, C.W. Zou, M. Li, D.J. Fu, Nucl. Inst. Methods B 262 (2007) 189.
[9] H.Y. Lee, W.S. Jung, J.G. Han, S.M. Seo, J.H. Kim, Y.H. Bae, Surf. Coat. Technol. 200 (2005) 1026.
[10] J.H. Jeon, S.R. Choi, W.S. Chung, K.H. Kim, Surf. Coat. Technol. 188 (2004) 415.
[11] Y. Cheng, Y.F. Zheng, Surf. Coat. Technol. 201 (2007) 6869.
[12] S. Gredelj, A.R. Gerson, S. Kumar, G.P. Cavallaro, Appl. Surf. Sci. 174 (2001) 240.
[13] M. Kumagai, K. Ogata, M. Kohata, K. Yamaguchi, Surf. Coat. Technol. 131 (2000) 187.
[14] J.T. Chen, J. Wang, F. Zhang, G.A. Zhang, X.Y. Fan, Z.G. Wu, P.X. Yan, J. Alloys Compd. 472 (2009) 91.
[15] G.S. Kim, B.S. Kim, S.Y. Lee, Surf. Coat. Technol. 200 (2005) 1814.
[16] B.Y. Man, L. Guzman, A. Miotello, M. Adami, Surf. Coat. Technol. 180 (2004) 9.
[17] O. Knotek, M. Bhmer, T. Leyendecker, J. Vac. Sci. Technol. 4 (1986) 2695.
[18] P.W. Shum, K.Y. Li, Y.G. Shen, Surf. Coat. Technol. 198 (2005) 414.
[19] G.S. Kim, S.Y. Lee, J.H. Hahn, Surf. Coat. Technol. 193 (2005) 213.
[20] A.H. Cottrell, An Introduction to Metallurgy, Edward Arnold, London, 1967.
[21] G.S. Kim, S.Y. Lee, J.H. Hahn, Thin Solid Films 506 (2006) 128.